Boundary-Layer Measurements on an Airfoil at Low Reynolds Numbers

M. Brendel* and T. J. Mueller†
University of Notre Dame, Notre Dame, Indiana

An experimental study was performed to investigate the characteristics of the transitional separation bubbles that form on the Wortmann FX63-137 airfoil at chord Reynolds numbers of 100,000, 150,000, and 200,000. Laser and hot-wire anemometry were used to obtain mean velocity profiles in the vicinity of the transitional bubble. A variety of basic parameters were calculated from these data with emphasis on possible biases introduced by the particular measurement technique. Of particular interest was the correlation of transition in the separated shear layer as a function of boundary-layer characteristics at separation. The transition Reynolds number was found to increase with the increasing momentum-thickness Reynolds numbers at separation. The momentum-thickness Reynolds numbers at separation ranged between 50 and 300. The results also suggested that the proximity of the separated shear layer to the airfoil surface influences the stability characteristics of the flow by inhibiting the formation of large vortical structures and subsequent pairing that have been shown to lead to turbulence in free shear flows.

Nomenclature

c = airfoil chord
h_b = height of separation bubble, $\sim\delta_{1t}-\delta_{1s}$
H_{12} = shape factor δ_1/δ_2
H_{32} = shape factor δ_3/δ_2
l_1 = laminar length of separation bubble
R_c = Reynolds number, chord, $U_\infty c/\nu$
R_{l1} = Reynolds number, transition, $U_{es}l_1/\nu$
$R_{\delta 2s}$ = Reynolds number, separation, $U_{es}\delta_{2s}/\nu$
Q = dynamic pressure
S = chordwise location of laminar separation
T = chordwise location of transition
TI = turbulence intensity, $\sqrt{u'^2}/U_\infty$
U,u = mean longitudinal reference and velocity, respectively
x = distance along chord
y = distance normal to surface
α = angle of attack
γ = separation angle, $\tan^{-1}[(\delta_{1t}\delta_{1s})/l_1]$
δ = boundary layer thickness
δ_1 = displacement thickness, $\int_0^\delta (1-u/U_e)\,dy$
δ_2 = momentum thickness, $\int_0^\delta (u/U_e)(1-u/U_e)\,dy$
ν = kinematic viscosity

Subscripts

e = external to boundary layer
s = separation
t = transition (max δ_1)
∞ = freestream condition

Introduction

THE performance of airfoils operating at chord Reynolds numbers below 500,000 has been of interest in modern subsonic aerodynamics.[1] Remotely piloted vehicles, sailplanes, human-powered vehicles, leading-edge control devices, high-altitude vehicles, wind turbines, and propellers are typical applications where low Reynolds numbers may be encountered. At higher Reynolds numbers, the boundary layer on the airfoil quickly becomes turbulent and is, in most cases, able to effectively negotiate the adverse pressure gradient downstream of the minimum pressure. In contrast, the boundary layer on a low Reynolds number airfoil often remains laminar well into the adverse pressure gradient region as shown in Fig. 1. In many cases, laminar separation takes place with transition to turbulence occurring in the separated shear layer. After transition, the energetic mixing causes the turbulent free-shear layer to reattach and develop as a turbulent boundary layer. This "closed" region is the transitional separation bubble. The presence of the bubble may significantly alter the predicted pressure distribution and, as a consequence, the performance of the airfoil. Hence, there has been increased interest in analytical and experimental investigations of the separation bubble in low-speed airfoil flows.[2-8] Transitional bubbles are known to occur at higher Reynolds numbers, but generally occupy less than 2% of the airfoil surface near the leading edge. As the chord Reynolds number decreases below about 300,000, the separation bubble may increase in length and often extend over 15% of the chord. Unfortunately, prediction of the formation and extent of the separation bubble has been a difficult problem, primarily because of incomplete understanding of the transition process.

In an effort to expand the experimental data base and extend the understanding of the transitional separation bubble, an experimental investigation was performed on the separation bubbles that occur on a Wortmann FX63-137 airfoil operating at low-chord Reynolds numbers. Discussion will focus on the several issues that have confronted researchers in the past, namely the effect of reverse flow on measurement of mean velocity profiles and the correlation of boundary-layer parameters with the occurrence of transition.

Single-sensor hot-wire velocity profiles, pressure distributions, flow visualization, and a limited set of laser velocimetry data were obtained for Reynolds numbers of 100,000, 150,000, and 200,000 and various angles of attack. Flow visualization was combined with hot-wire velocity measurements to study the separation location and shear layer trajectory. The variety of measurement techniques were intended to be complimentary and aid in identifying potential probe-boundary layer interaction.

Experimental Apparatus

All data were obtained in a Notre Dame subsonic, open-return, indraft wind tunnel. The tunnel consists of four

Received Dec. 21, 1986; presented as Paper 87-0495 at the AIAA 25th Aerospace Sciences Meeting, Reno, NV, Jan. 12-15, 1987; revision received Sept. 23, 1987.

*Research Associate, Department of Aerospace and Mechanical Engineering; currently Assistant Professor, Florida Institute of Technology, Melbourne, FL, Member AIAA.

†Professor, Department of Aerospace and Mechanical Engineering. Associate Fellow AIAA.

basic components: a 24 : 1, three-dimensional, inlet contraction with 12 antiturbulence screens; an interchangeable 0.61 m × 0.61 m × 2 m (24 in. × 24 in. × 72 in.) long working section; a 4.2 m long diffuser with 4.2 deg included angle divergence; and an 18.6 kW ac motor directly coupled to a 1.2 m (48 in.) diam fan. The measured turbulence (disturbance) levels, using a single-sensor hot-wire, were less than 0.08% for a 1–2500 Hz bandwidth and less than 0.025% for 25–2500 Hz bandwidth. Spectra did not reflect a turbulence character; hence, acoustic influences probably dominated at these low levels. Several peaks in the spectra could be correlated with fan blade passage frequencies and electronic noise, although these were several orders of magnitude below the major constituents of the spectrum.

The test section had a computer-controlled traversing mechanism for moving the hot-wire sensor in the streamwise and vertical directions. The entire probe holder mechanism could be manually rotated in the traversing plane in order to change the sensor angle relative to the airfoil surface. The traversing mechanism had a resolution of 0.006 mm (0.0003 in.) in the streamwise direction, 0.02 mm (0.001 in.) in the vertical direction, and 0.5 deg in rotation.

Several cast epoxy Wortmann FX63-137 airfoils were used in this study; a 152 mm (6 in.) chord model with 40 pressure taps, a 305 mm (12 in.) chord model with 96 pressure taps, and a 305 mm (6 in.) chord model for hot-wire measurements and flow visualization. All airfoils had a span of about 400 mm (16 in.) and were mounted between two endplates in the test section. Comparison of pressure distributions from the two different chord models was used to determine the severity of solid blockage in the wind tunnel. The differences were within the experimental uncertainty for angles of attack less than 10 deg. All hot-wire surveys were performed on the larger model (305 mm chord) to take advantage of the thicker boundary layer chord for a given Reynolds number.

Hot-wire measurements were obtained with a constant temperature anemometer and a standard single-sensor boundary-layer probe. The anemometer output was calibrated in situ against a pitot static tube and then fitted to a fourth-order polynomial. A 4 W argon-ion laser, a counter, and a frequency shifter were used for laser velocimetry (LV) measurements. The laser was operated in forward scatter mode with frequency shifts of 0.5 to 1.0 MHz. The entire system was mounted on a modified milling machine and could be manually traversed with a least count of 0.025 mm (0.001 in.) in three directions. All data acquisition and processing were performed on a laboratory minicomputer. Further details of the apparatus and techniques may be found in Ref. 9.

Results

Details for two cases, −5 and 7 deg, at a nominal-chord Reynolds number of 100,000 are presented here. A summary of pertinent boundary-layer parameters for all tests, including laser velocimetry measurements, are given in Table 1. A brief discussion of these results and the methods in which they were obtained are given with particular attention to the influence of reverse flow on the integrated boundary-layer parameters and to the transition Reynolds number R_{l1}.

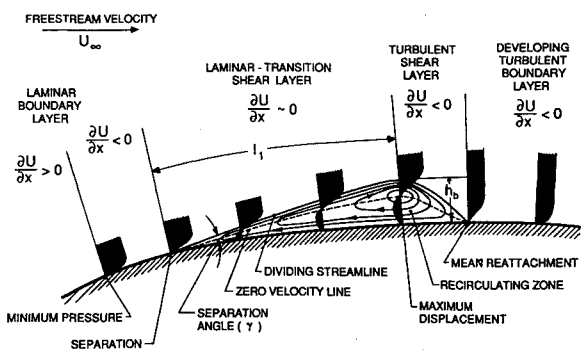

Fig. 1 Mean features of the boundary layer on a low Reynolds number airfoil.

Hot-Wire Velocity Profiles

Figures 2 and 3 are plots of the longitudinal velocity profiles at −5 and 7 deg angles of attack. Lines of constant velocity, nondimensionalized with the local external velocity, are provided as a reference to show the general character of the laminar separation bubble. (The profiles are stretched normal to the surface by a factor of 3 to enhance detail.) Each of the 40 points describing the profile is an average of 512 samples obtained over a period of about 5 s. The location of laminar separation, the onset of transition, and reattachment are indicated in the plot. To establish these locations, several data processing criteria were applied in a uniform manner such that all the present data could be compared in a consistent manner. These criteria will be discussed below.

"Integrated" boundary-layer thicknesses, displacement δ_1, and momentum δ_2, as functions of chordwise position are shown in Figs. 4 and 5. The displacement thickness gradient increases just after separation whereas the momentum thickness continues to increase at approximately the same rate as before separation. This demonstrates that stresses in the fore portion of the bubble are predominately due to viscosity and do not promote rapid diffusion of momentum. At some distance downstream, the separated shear layer undergoes transition, due to the roll-up and breakdown of the separated shear layer, which causes a marked increase in the momentum and energy thickness gradients. Although the presence of reverse flow, particularly near the aft portion of the separated region, will influence these values, the general character of the separation bubble was well represented by the hot-wire results.

The directional ambiguity of the single-sensor hot-wire precludes detection of reverse flow. A standard crossed-wire probe would have been too large to obtain reasonable results since the scale of the flow was of same order as the sensors (~ 2 mm). Since the single-sensor probe rectifies the measured velocity, the calculation of the integrated boundary-layer parameters is subject to error. The relative magnitude of the error can be shown in a simple analysis of the velocity profiles from reverse flow solutions to the Falkner-Skan equation. A comparison of the integrated thicknesses using these velocity profiles and those obtained using the absolute value of the same velocity profiles (a simplified hot-wire approximation) can, at least, give some indication of the magnitude of the errors present in the hot-wire data.[6] Results show that the displacement thickness calculated from the hot-wire data should be less than the actual value, but the relative error is negligible compared to error in the momentum thickness in the presence of strong reversed flow. As an example, the momentum thickness calculated from the hot-wire may be as much as 250% greater than the actual value when the maximum reverse flow is on the order of 10% of the external velocity. In contrast, the displacement thickness is about 10% lower than the actual value. Hence, the calculated values of H_{12} will tend to be underestimated in regions with reverse flow. The question remains as to the extent of the reverse flow in actual separation bubbles in order to evaluate the single-sensor hot-wire data.

Laser Velocimetry

The laser velocimeter was used to repeat the −5 and 7 deg cases at a Reynolds number of 100,000. Figures 6 and 7 compare the hot-wire and laser anemometer profiles in the vicinity of the separation bubble. In addition to reverse flow measurements, these data were intended to identify possible probe interference. It has been found that the flow in the vicinity of the separation bubble could be influenced by the presence of the hot-wire sensor and holder.[9,10] These studies suggested that the angle between the surface tangent and the sensor was an important factor. In general, angles less than 10 deg appeared to have little to no influence.

Table 1 Separation bubble parameters, Wortmann FX63-137

Angle of attack surface, nominal R_c	−5 deg Upper 100 k	−5 deg Lower 100 k	0 deg Upper 100 k	0 deg Lower 100 k	3 deg Upper 100 k	7 deg Upper 100 k	7 deg Upper 150 k	7 deg Upper 200 k	15 deg Upper 100 k	7 deg Upper 100 k LV
S, % chord	65	2	53	41	42	33	33	34	7	33
T, % chord	92	10.3	78	66	69	53	53	50	17	53
l_b, % chord	26.6	8.2	24.9	24.9	8.2	20.3	20.3	16.1	10.2	20.0
h_b, % chord[a]	1.6	0.9	1.9	1.5	1.8	1.0	0.6	0.3	0.6	1.0
γ, deg	3.6	5.8	4.3	3.4	3.7	3.0	1.6	1.2	3.2	2.8
$R_{l1} \times 10^{-3}$	33 ± 2	13.5 ± 2	33 ± 2	27 ± 2	41 ± 2	33 ± 3	51 ± 4	56 ± 5	19 ± 3	31 ± 3
δ_1, % chord	0.62	0.10	0.43	0.52	0.39	0.36	0.26	0.26	0.23	0.39
δ_2, % chord	0.16	0.03	0.14	0.16	0.13	0.11	0.10	0.08	0.07	0.12
$R_{\delta 1s}$	760 ± 50	159 ± 53	573 ± 48	587 ± 46	609 ± 52	586 ± 55	646 ± 83	885 ± 114	440 ± 63	597
$R_{\delta 2s}$	194 ± 9	50 ± 5	182 ± 8	176 ± 9	194 ± 7	188 ± 7	236 ± 9	281 ± 11	127 ± 7	180
H_{12s}	3.85	3.11	3.14	3.32	3.15	3.12	2.74	3.15	3.47	3.33
H_{32s}	1.54	1.53	1.54	1.54	1.54	1.54	1.55	1.54	1.52	1.56
δ_{1t}, % chord	2.26	0.95	2.30	2.00	2.16	1.41	0.82	0.59	0.79	1.38 (1.34)[b]
δ_{2t}, % chord	0.56	0.12	0.28	0.27	0.35	0.20	0.18	0.12	0.14	0.22 (0.25)[b]
$R_{\delta 1t}$	2727 ± 120	1445 ± 62	2926 ± 114	2113 ± 11	3084 ± 100	2182 ± 73	2023 ± 83	2008 ± 11	1477 ± 66	2136
$R_{\delta 2t}$	666 ± 28	193 ± 7	352 ± 13	286 ± 15	503 ± 15	311 ± 16	433 ± 9	426 ± 11	260 ± 73	345
H_{12t}	4.09	7.50	8.31	7.40	6.13	7.03	4.67	4.71	5.69	6.21
H_{32t}	1.37	1.34	1.41	1.48	1.37	1.45	1.43	1.49	1.38	1.49
δ_{1t}/δ_{2s}	14.1	31.6	16.4	12.5	16.6	12.8	8.2	7.3	11.3	11.5

[a]Defined as $\tan^{-1}[(\delta_{1t} - \delta_{1s})/l_l]$ except for LV, where it is defined as the slope of the dividing streamline.
[b]Values obtained when absolute value of LV velocity is integrated.

Uncertainty notes

Value:	Uncertainty:	Source:
Location of laminar separation, S	±0.5% chord	Flow visualization
Location of transition, T	±1.5% chord	Hot-wire data spacing
Displacement thickness, δ_1	±0.03% chord (typical)	Probe-surface distance
Momentum thickness, δ_2	±0.003% chord (typical)	Probe-surface distance

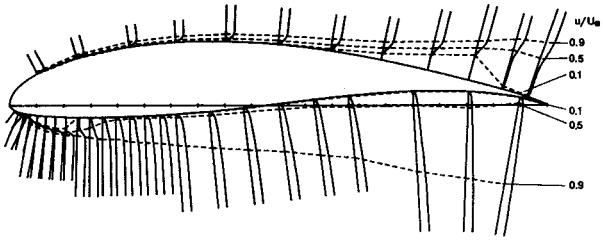

Fig. 2 Boundary velocity profiles (hot-wire) on the Wortmann FX63-137 airfoil: $R_c = 100{,}000$ $\alpha = -5$ deg; $c = 305$ mm (normal scale expanded ×3).

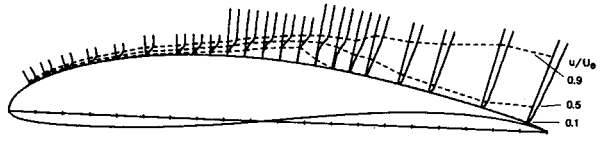

Fig. 3 Boundary velocity profiles (hot-wire) on the Wortmann FX63-137 airfoil: $R_c = 100{,}000$: $\alpha = 7$ deg; $c = 305$ mm (normal scale expanded ×3).

Differences between the hot-wire and LV velocity profiles in the laminar portion of the separation bubble stem from several causes. The most influential is the uncertainty in sensor position relative to the surface. Placement of the sensor above the surface is estimated to be uncertain by 0.1 mm for the hot-wire and 0.2 mm for the LV. This uncertainty has the greatest influence in the calculation of displacement thickness, but little effect on momentum and energy thickness since the uncertainty in the distance between data points is about an order of magnitude less than the absolute distance. Downstream of transition, both sets of data show some discrepancies. Flow visualization showed that reattachment was an unsteady phenomenon and tended to move periodically about a mean location. Hence, an intermittent reverse flow could result in a relatively large positive bias to the single-sensor hot-wire, and disagreement between the two techniques is expected. This appears to be the situation for the −5 deg case. In contrast, the 7 deg case has the opposite discrepancy. Another consideration is that the LV data represent the velocity vector tangent to the surfce. Flow curvature, the influence of a v-component, will alter the comparison.

In any event, the comparison between the hot-wire and the LV shows that the physical presence of the probe did not measurably alter the character of the flow in the laminar portion of the bubble. Further, the maximum reverse flow never exceeded 10% (typically 5%) of the external velocity in the cases studied. As expected, the displacement thickness was influenced very little, relative to the momentum thickness, by the two measurement methods. The momentum thickness growth in the laminar portion of the bubble, as calculated with the LV data, was not significantly different from the hot-wire value for the 7 deg case. However, larger reverse flow velocities were detected in the −5 deg case and are reflected in the large difference in momentum thickness at transition δ_{2t} between the hot-wire and LV measurements. In Table 1, LV data processed to simulate the hot-wire, by taking the absolute value of velocity, are shown in parenthesis. Although the directional ambiguity of the hot-wire has a major impact on the calculation of boundary-layer parameters, significant observations concerning the laminar separation bubble may still be deduced.

The character of the boundary layer at separation, such as the momentum thickness Reynolds number $R_{\delta 2s}$, has been of

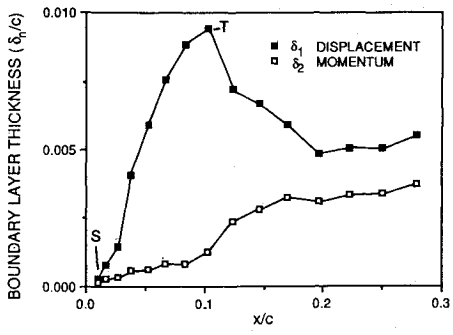

Fig. 4 Integrated boundary-layer parameters on the Wortmann FX63-137 airfoil, lower surface: $R_c = 100{,}000$; $\alpha = -5$ deg; $c = 305$ mm.

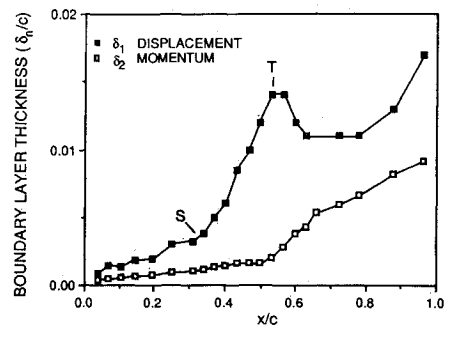

Fig. 5 Integrated boundary-layer parameters on the Wortmann FX63-137 airfoil, upper surface: $R_c = 100{,}000$; $\alpha = 7$ deg; $c = 305$ mm.

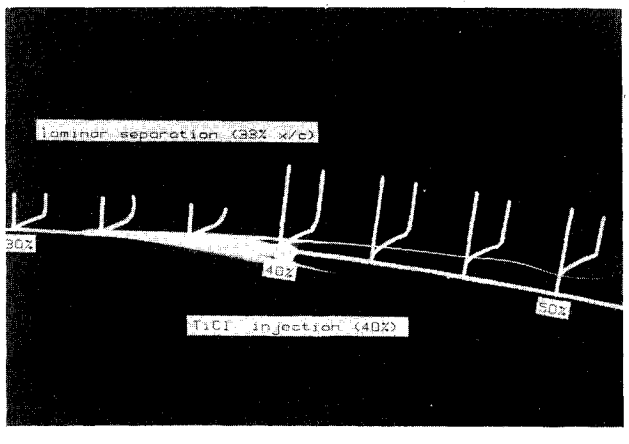

Fig. 6 Comparison of velocity profiles obtained by the hot-wire and laser velocimeter. Wortmann FX63-137 airfoil, lower surface: $R_c = 100{,}000$; $\alpha = -5$ deg; $c = 305$ mm.

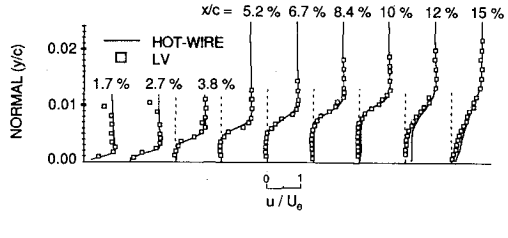

Fig. 7 Comparison of velocity profiles obtained by the hot-wire and laser velocimeter. Wortmann FX63-137 airfoil, upper surface: $R_c = 100{,}000$; $\alpha = 7$ deg; $c = 305$ mm.

most interest in correlations of separation bubble development. The state of the boundary layer at separation represents the history of the boundary layer and should, in part, be critical in determining events that occur downstream. In order to establish some correlations that were not influenced by reverse flow, the locations of separation and transition were obtained from a combined evaluation of hot-wire data and flow visualization.

Laminar Separation

The location of separation was determined from both the hot-wire profiles and flow visualization. Lines of constant velocity magnitude were extrapolated from profiles within the laminar portion of the bubble to intersect with the airfoil surface. The mean intersection based on several least-square curve fits of velocity ratios between 0.1 and 0.2 were found to agree with titanium tetrachloride flow visualizations to within 1% of chord length. It is interesting to note that the Falkner-Skan reverse flow profiles with reverse flow magnitudes similar to those observed in the LV data have a velocity ratio at the dividing streamline between 0.1 and 0.2. Figure 8 is a flow visualization of the separation bubble at 7 deg angle of attack superimposed with the velocity profiles obtained from the hot-wire. Titanium tetrachloride was injected into the laminar portion of the bubble at 40% of chord. The white "smoke" (titanium dioxide) then flowed upstream in the recirculating region and then separated from the airfoil surface at about 33% of the chord. The fineness of the filament again shows the weak diffusion in the laminar portion of the bubble. The comparison between velocity profile and flow visualization is not valid in the vicinity of the shear layer roll-up since the hot-wire is a time-averaged representation while the flow visualization is approximately instantaneous (20 μs). Real-time observation of the flow indicated that the reverse flow was on the order of cm/s. Laser velocimetry measurements confirmed this. In general, the location of separation was between hot-wire traversing stations, therefore, boundary-layer parameters at separation, presented in Table 1, were determined by linear interpolation.

Transition

Although transition does not occur at a fixed location, the rapid roll-up of the shear layer appears as a sharp decrease in displacement thickness coincident with a sharp increase in momentum thickness. Therefore, the transition was simply defined as the location where the bubble reached its maximum displacement from the surface. This could easily be seen in the hot-wire data, even though the presence of reverse flow would alter the numerical value of the displacement thickness. The criterion has an inherent uncertainty of $\pm 1.5\%$ of chord since this represents one-half the chordwise spacing of the velocity profiles. Velocity spectra were obtained for several cases to justify this approximation.

Figures 9 and 10 are velocity spectra obtained at several chordwise stations before and after laminar separation. The spectra have a bandwidth of 40 to 2500 Hz and were obtained at a point in the shear layer where the velocity was one-half that of the external flow. A band of unstable frequencies appears to amplify in the layer as would be expected from linear stability theory. Finally, a broadband turbulent spectrum emerges in the vicinity of maximum displacement. The change

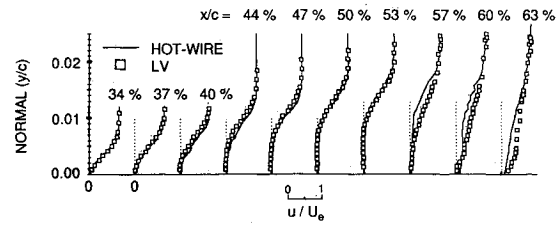

Fig. 8 Titanium tetrachloride flow visualization superimposed on measured velocity profiles (hot-wire) on the Wortmann FX63-137 airfoil: $R_c = 100{,}000$, $\alpha = 7$ deg; $c = 305$ mm.

in spectral shape illustrates the rapidity of the transition process and further suggests that maximum displacement represents a gross change in the character of the flow. The growth of disturbances in the separated shear layer is exponential. Although transition occurs well before the location maximum displacement, its presence is not detectable in a mean velocity profile.

Transition Reynolds Number

In order to predict accurately the state of the boundary layer downstream of the transitional separation bubble, one must be able to predict transition. Since there is no theory for transition, empirical methods have been attempted in the past. Typically, a common parameter has been the transition Reynolds number, R_{tl}. The transition Reynolds number may be used to determine the length of the laminar portion of the bubble as a function of conditions at separation (assumed to be known a priori). Many early studies of transitional bubbles suggested that transition Reynolds number was a constant. In the present data, R_{tl} ranged between 13,500 and 56,000 and tended to increase with increasing $R_{\delta 2s}$. This appeared to hold for changes in both chord Reynolds number and angle of attack. As listed in Table 1, the comparison of the 7 deg case for R_c of 100,000, 150,000, and 200,000 shows that the increase in external velocity at separation dominated the decrese in transition length (if any could be detected within the uncertainty band). For a Reynolds number independent pressure distribution, the external velocity at separation increases in proportion to the chord Reynolds number, while the momentum thickness is inversely proportional to the square root of the chord Reynolds number. Ultimately, this results in $R_{\delta 2s} \sim R_c^{1/2}$. Separation occurs at nearly the same location for the three chord Reynolds numbers, indicating similar pressure distributions. Thus, the observed relation between separation Reynolds number and chord Reynolds number is expected, but this does not imply a simple dependence of R_c on R_{tl}. The correlation between R_{tl} and $R_{\delta 2s}$ is shown in Fig. 11 for all the present data along with data from two other recent airfoil experiments. One set of data was obtained from a NACA 66_3-018 airfoil at R_c ranging from 30,000 to 160,000 with angles of attack of 10 and 12 deg.[7] The second source of data was obtained from a Wortmann FX63-137 airfoil at chord Reynolds numbers of 150,000 to 250,000 with angles of attack of 12 and 14 deg.[8] A variety of chord Reynolds numbers and incidence angles are represented by the correlation in the figure.

The increase in R_{tl} with increasing $R_{\delta 2s}$, probably does not continue indefinitely since this would imply that laminar separation (at a fixed location) always occurs. As one increases the chord Reynolds number, the location of transition will eventually move upstream as the boundary layer Reynolds number attains the critical value for transition prior to laminar separation. A limiting value of R_{tl} may be suggested by Fig. 11, but there are insufficient data above $R_{\delta 2s} = 300$ to be conclusive. The trend in the data does warrant further comment.

The proximity of the separated shear layer to the airfoil surface can have an influence on the stability characteristics of the flow.[11] In general, it was observed that the angle at which the layer leaves the surface, γ, at separation varied inversely to $R_{\delta 2s}$. This has been shown analytically in the vicinity of separation[12] although the proportionality does not appear to be constant in the present data. Roughly, one can consider the ratio δ_{1t}/δ_{2s} as representing the proximity of the separated shear layer to the surface, cast in terms of the momentum thickness at separation. As shown in the table, increasing R_{tl} corresponds to a decreasing value of δ_{1t}/δ_{2s}, suggesting a damping effect on the shear layer roll-up when its trajectory was near to the wall. Whereas the separated shear layer in the 7 deg ($R_{tl} = 33{,}000$) case may be physically farther from the wall than the -5 deg ($R_{tl} = 13{,}500$) case, the distance in terms of momentum thickness is the opposite. In general, lower $R_{\delta 2s}$ corresponds to separated flows that approximate free shear layers. These are less stable than the wall bounded counterpart.

Figure 11 may be recast in terms of $1/R_{\delta 2s}$ (proportional to shear layer trajectory angle) as shown in Fig. 12. A lower limit of R_{tl} is suggested as the separated shear layer becomes more like a free shear layer. In other words, the initial roll-up of the fundamental instability of the separated shear layer may saturate early due to the presence of the surface and vortex pairing,

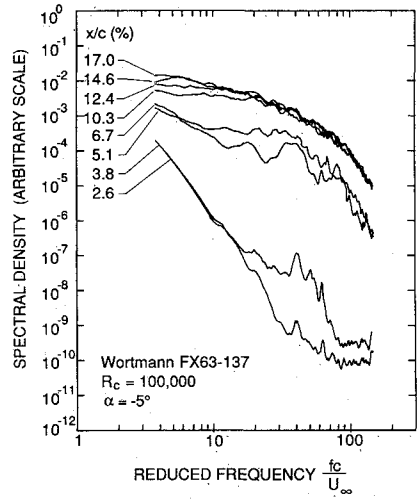

Fig. 9 Velocity spectra obtained in the separated shear layer on the Wortmann FX63-137 airfoil, lower surface: $R_c = 100{,}000$; $\alpha = -5$ deg; $c = 305$ mm.

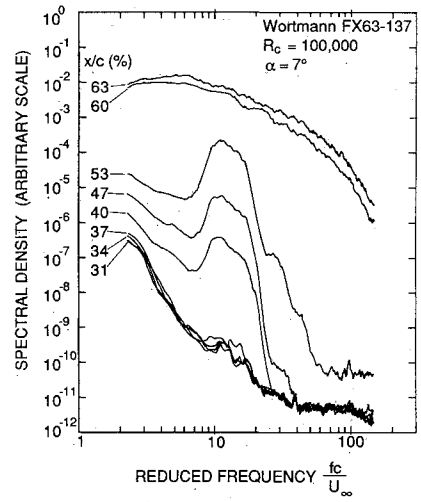

Fig. 10 Velocity spectra obtained in the separated shear layer on the Wortmann FX63-137 airfoil, upper surface: $R_c = 100{,}000$; $\alpha = 7$ deg; $c = 305$ mm.

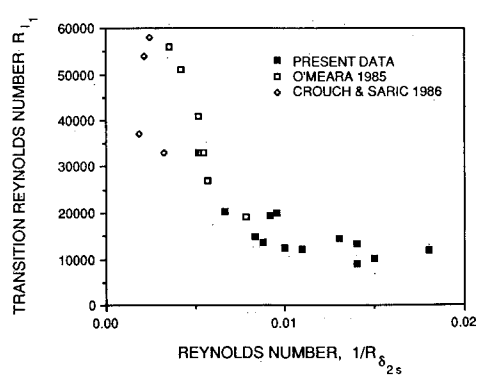

Fig. 11 Transition Reynolds number R_{t_1} vs momentum Reynolds number at separation $R_{\delta 2s}$.

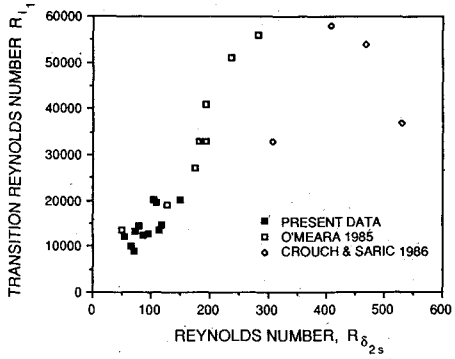

Fig. 12 Transition Reynolds R_{l_1} number vs the inverse momentum Reynolds number at separation $1/R_{\delta 2s}$.

which aids in further breakdown to turbulence, fails to take place.

Transition is also influenced by the magnitude of freestream disturbances. Typically, the measured rms velocity fluctuation (turbulence intensity) in the freestream has been used as the measure of disturbances and sometimes used to correlate transition phenomena. An increase in turbulence intensity should, in some way, be associated with a decrease in transition Reynolds number (or transition length, l_1). The important experiments of Schubauer and Skramstad on boundary-layer transition elude to the problems associated with turbulence intensity correlations.[13] While an increase in turbulence intensity will usually decrease the transition Reynolds number, the composition of the frequency spectrum with regard to boundary layer receptivity is the key correlation. Measured turbulence intensities less than 0.1% are predominately comprised of acoustic phenomena, hence, not really turbulence. In addition, the spectra may show little energy in frequencies that correspond to the shear layer instability and thus the effect on the transition process may not be as severe as indicated by turbulence intensity alone. For instance, an acoustic excitation at the fundamental frequency of the separated shear layer may promote transition earlier than a corresponding flow with identical turbulence intensity but different spectral composition. Likewise, disturbances effecting the flow upstream of separation must also be considered. The scatter in Figs. 11 and 12 probably represents a combination of external influences. The probe interference, wind tunnel fan noise, noise generated by the wind tunnel boundary walls, or noise generated at the trailing edge of the airfoil model can contribute. Likewise, disturbances originating with the flight behicle may influence the boundary layer. The data presented here represent two different wind tunnels with measured turbulence intensities reportedly ranging from 0.02% to 0.2%. (Some of the data of Ref. 7 were obtained with a flow restrictor placed downstream of the model. The increase in fan speed required to produce the same Reynolds number as without the restrictor increased the measured disturbance level.) It appears that the influence of freestream disturbances in low turbulence wind tunnels is difficult to correlate to transition in separation bubbles.

Conclusions

An experimental study of the boundary layer on a low Reynolds number airfoil has been undertaken. Pressure distributions, hot-wire and laser velocimeter velocity profiles, and flow visualization have been used to study the transitional separation bubbles that occur at low-chord Reynolds numbers. Hot-wire and laser velocimetry data comparisons show little evidence of probe interference provided the hot-wire sensor approaches the surface at an angle of 10 deg or less. The maximum reverse flow within the separation bubble was typically 5% of the external flow for the conditions studied. In cases with larger reverse flow, the momentum and energy thicknesses are significantly overestimated by the hot-wire data. However, the important characteristics of the separation bubble could still be extracted. Transition Reynolds numbers R_{l1} were found to increase with increasing momentum thickness Reynolds number at separation, $R_{\delta 2s}$ in the range of about 50 to 350. The proximity of the separated shear layer to the wall and its effect on stability appears to be reflected in the range of R_{l1} which was found to decrease with increasing displacement of the separated shear layer from the wall, measured in terms of momentum thickness. External influences, such as disturbance environment, were not obvious in the present data.

Acknowledgments

This work was supported by the Office of Naval Research under contract N00014-83-K-0239, and the Department of Aerospace and Mechanical Engineering, University of Notre Dame.

References

[1]Mueller, T. J., "Low Reynolds Number Vehicles," AGARDograph 288, Feb. 1985.

[2]Gaster, M., "The Structure and Behavior of Laminar Separation Bubbles," AGARD Conference Proceedings No. 4, 1966, pp. 813–854.

[3]Horton, H. P., "A Semi-empirical Theory for the Growth and Bursting of Laminar Separation Bubbles," Aeronautical Research Council CP 1073, 1967.

[4]Roberts, W. B., "Calculation of Laminar Separation Bubbles and Their Effect on Airfoil Performance," AIAA Paper 79-0285, 1979.

[5]*Proceedings of the Conference on Low Reynolds Number Airfoil Aerodynamics*, edited by T. J. Mueller, University of Notre Dame, Notre Dame, IN, UNDAS-CP-77B123, 1985.

[6]Schmidt, G. S., "The Prediction of Transitional Separation Bubbles at Low Reynolds Numbers," Ph.D. Thesis, University of Notre Dame, Notre Dame, IN, May 1986.

[7]O'Meara, M. M. and Mueller T. J., "Experimental Determination of the Laminar Separation Bubbles on the Airfoil at Low Reynolds Numbers," *AIAA Journal*, Vol. 25, Aug. 1987, pp. 00–00.

[8]Crouch, J. D. and Saric, W. S., "Oscillating Hot-Wire Measurements Above an FX63-137 Airfoil," AIAA Paper 86-0012, Jan. 1986.

[9]Brendel, M. "Experimental Study of the Boundary Layer on a Low Reynolds Number Airfoil in Steady and Unsteady Flow," Ph.D. Thesis, University of Notre Dame, Notre Dame, IN, May 1986.

[10]Huber, A. F., "The Effects of Roughness on an Airfoil at Low Reynolds Numbers," Master's Thesis, University of Notre Dame, Notre Dame, IN, May 1985.

[11]Betchov, R. and Criminale, W. O., *Stability of Parallel Flows*, Academic Press, New York, 1967, p. 83.

[12]Van Ingen, J. L. and Boermans, L. M. M., "Research on Laminar Separation Bubbles at Delft University of Technology in Relation to Low Reynolds Number Airfoil Aerodynamics", *Proceedings of the Conference on Low Reynolds Number Airfoil Aerodynamics*, Notre Dame, IN, June 1985, pp. 89–124.

[13]Schubauer, G. B. and Skramstad, H. K., "Laminar Boundary Layer Oscillations and Transition on a Flat Plate," NACA TR 909, 1948.